

Ligand-Guided Investigation of a Series of Formamidine-Based Thiuram Disulfides as Potential Dual-Inhibitors of COX-1 and COX-2

Segun D. Oladipo,^{*a, b} Olayinka I. Akinpelu,^c and Bernard Omondi^{*a}

^a School of Chemistry and Physics, Westville Campus, University of Kwazulu-Natal, Private Bag X54001, Durban, 4000, South Africa, e-mail: owaga@ukzn.ac.za; oladipodanielsegun@gmail.com

^b Department of Chemical Sciences, Olabisi Onabanjo University, P.M.B 2002, Ago-Iwoye, Nigeria

^c Department of Biochemistry, Genetics and Microbiology, Faculty of Natural Science, University of Pretoria, Private Bag X20, Hatfield 0028, South Africa

© 2022 The Authors. Chemistry & Biodiversity published by Wiley-VHCA AG. This is an open access article under the terms of the Creative Commons Attribution Non-Commercial License, which permits use, distribution and reproduction in any medium, provided the original work is properly cited and is not used for commercial purposes.

A series of thiuram disulfides **1–6** which had been previously synthesized and characterized,^[1] were studied for their potential therapeutic properties. Target-fishing analyses through HitPick and SwissTarget prediction identified COX1 and COX2, which are essential biomolecules in cancer-related inflammations, as the possible targets for compounds **1** and **4** among all the compounds tested. These two proteins have enjoyed interest as targets for treating some neoplastic cancer types such as breast, colorectal, skin, pancreatic, haematological and head cancers. The inhibitory potency of **1** and **4** as lead anticancer drug candidates with dual-target ability against COX1 and COX2 was examined through molecular docking, molecular dynamics simulation and post-MD analyses such as binding energy calculation, RMSD, RMSF, and RoG. The two compounds had better docking scores and binding energies than the known inhibitors of COX1 and COX2. Insights from the RMSD, RMSF, and RoG suggested that both **1** and **4** showed observable influence on the structural stability of these targets throughout the simulation. The reported observations of the effects of **1** and **4** on the structures of COX1 and COX2 indicate their probable inhibitory properties against these target proteins and their potential as lead anticancer drug candidates.

Keywords: thiuram disulfide, cyclooxygenase 1 and 2, molecular docking, binding energy.

1. Introduction

Chemical synthesis is an essential part of the drug discovery process.^[1] Therefore, the ability to synthesize new chemical entities with possible activities against pathologic druggable protein targets could significantly contribute to translational therapeutic interventions across various diseases.^[2–4] A series of formamidine-based thiuram disulfide compounds (Figure 1) synthesized by our group had been reported in some of our previous publications.^[1,5] They were synthesized via iodine oxidation of dithiocarbamates salts following a known protocol.^[1,6] In summary, 2 mmol of potassium *N,N*-diarylformamidine dithiocarbamate salts reacted with 1 mmol of iodine to afford the respective formamidine-based thiuram disulfide. The reported

compounds showed moderate antimicrobial activities against Gram-negative bacteria. In silico pharmacokinetic prediction revealed the druggability of these compounds, further supporting their potential to evolve into future therapeutic drugs. While the initial studies on these compounds focused more on exploring their antimicrobial activities, there are high possibilities of other innate and interesting pharmacological tendencies for further exploration.

Computer-aided methods have been utilized extensively in drug discovery since 1980,^[7] and have helped to speed up and provide a feasible strategy for drug development. A boom in multi-omics data and advancements in computational techniques have improved the development of various cheminformatics, pharmacoinformatic and bioinformatic tools used in drug discovery.^[8] Ligand-target inter-

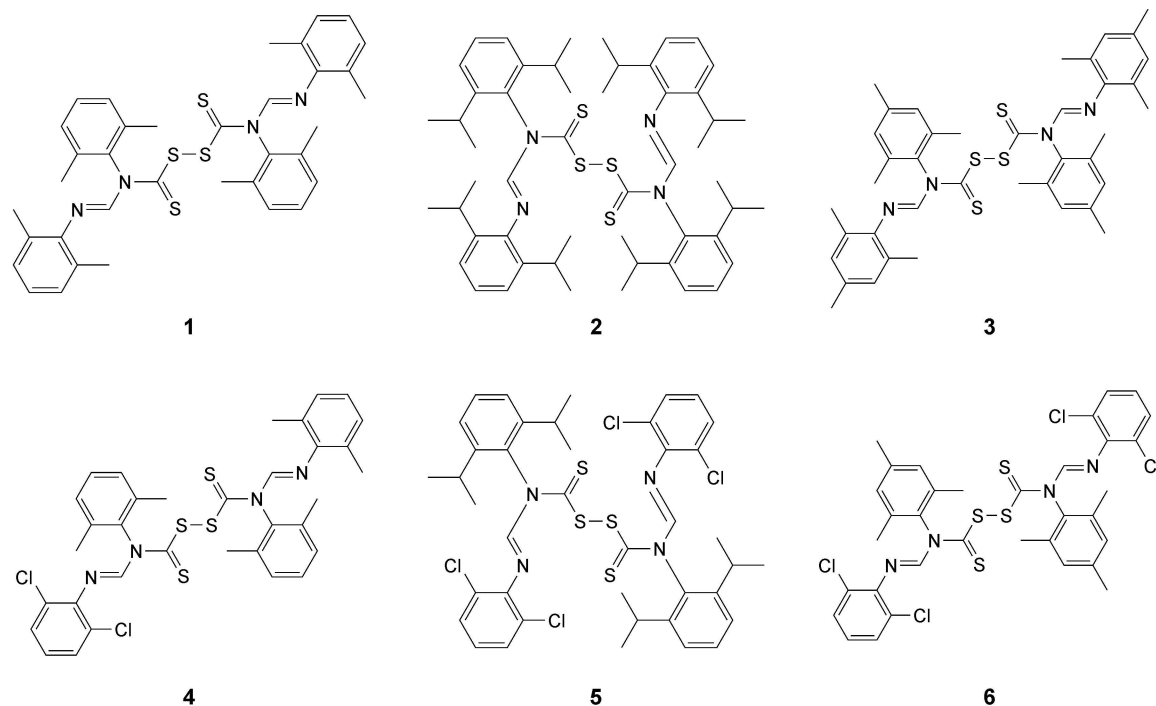


Figure 1. 2D structures of formamidine based thiuram disulfides.

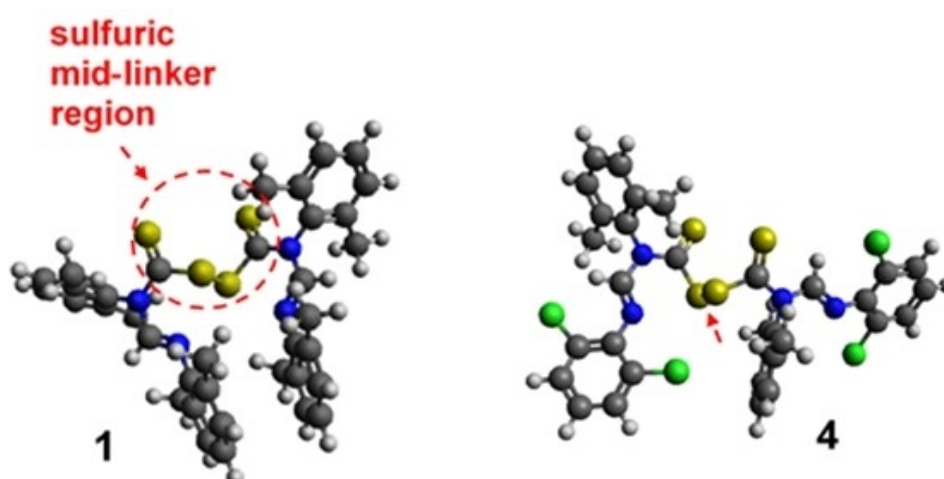


Figure 2. Structural and geometrical optimization of the **1** and **4**.

action and binding are some of the bedrock of conventional drug design and development.^[9] Computational methods such as Molecular docking and Molecular dynamics (MD) simulations are some of the techniques for studying these target-ligand complex interactions.^[10–13] While molecular docking is a preliminary approach to obtain essential insight into the binding poses and interactions that suggest potential therapeutic inhibitors. MD is a technique

that simulates the dynamic behaviour of molecules (usually enclosed in a box) as a function of time.^[14]

In this study, we employed combinatorial Computer-Aid Drug Design (CADD) methods to mine for possible biomolecular targets implicated in disease development for which the formamidine-based thiuram disulfide could serve as potential drugs. The preliminary target identification study suggested COX1 and COX2 as the potential targets for **1** and **4**. COX1 and COX2 have been identified as druggable

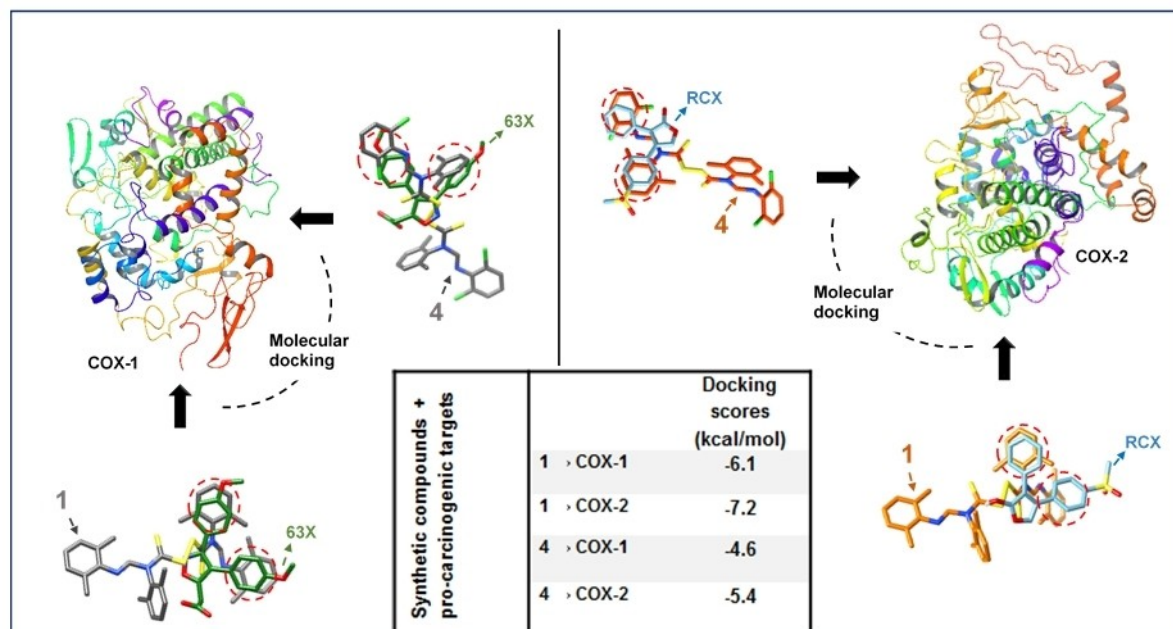


Figure 3. Docking poses and corresponding scores of **1** and **4** to COX1/2. Also shown is the superposition of the **1** and **4** with co-crystallized COX1/2 ligands retrieved from PDB. 63X is COX-1 co-crystallized ligand, while it is RCX for COX-2. Ring alignment between these compounds and the co-crystallized compounds are highlighted in dashed-red circles. These were obtained by post-docking active site superimposition.

targets in many cancer types. COX1 is known to be an essential enzyme regulating the production of PGE₂ in ovarian cancer cells.^[15] COX1 and COX2 are responsible for the migration and invasion of gonadotropin-induced tumor cells.^[16] A well-known inhibitor of COX1 is mofezolac (63X), a nonsteroidal anti-inflammatory drug (NSAID) while COX2 known inhibitor is rofecoxib (RCX).^[17] Both RCX and 63X have been observed to cause several side effects. RCX was discontinued after 5 years of approval due to adverse cardiovascular effects on patients. 63X is also known to cause gastrointestinal problems, oedema, erythema, and rash. Therefore, the need to discover new drugs which can inhibit COX1 and COX2 with minimal or no side effects.

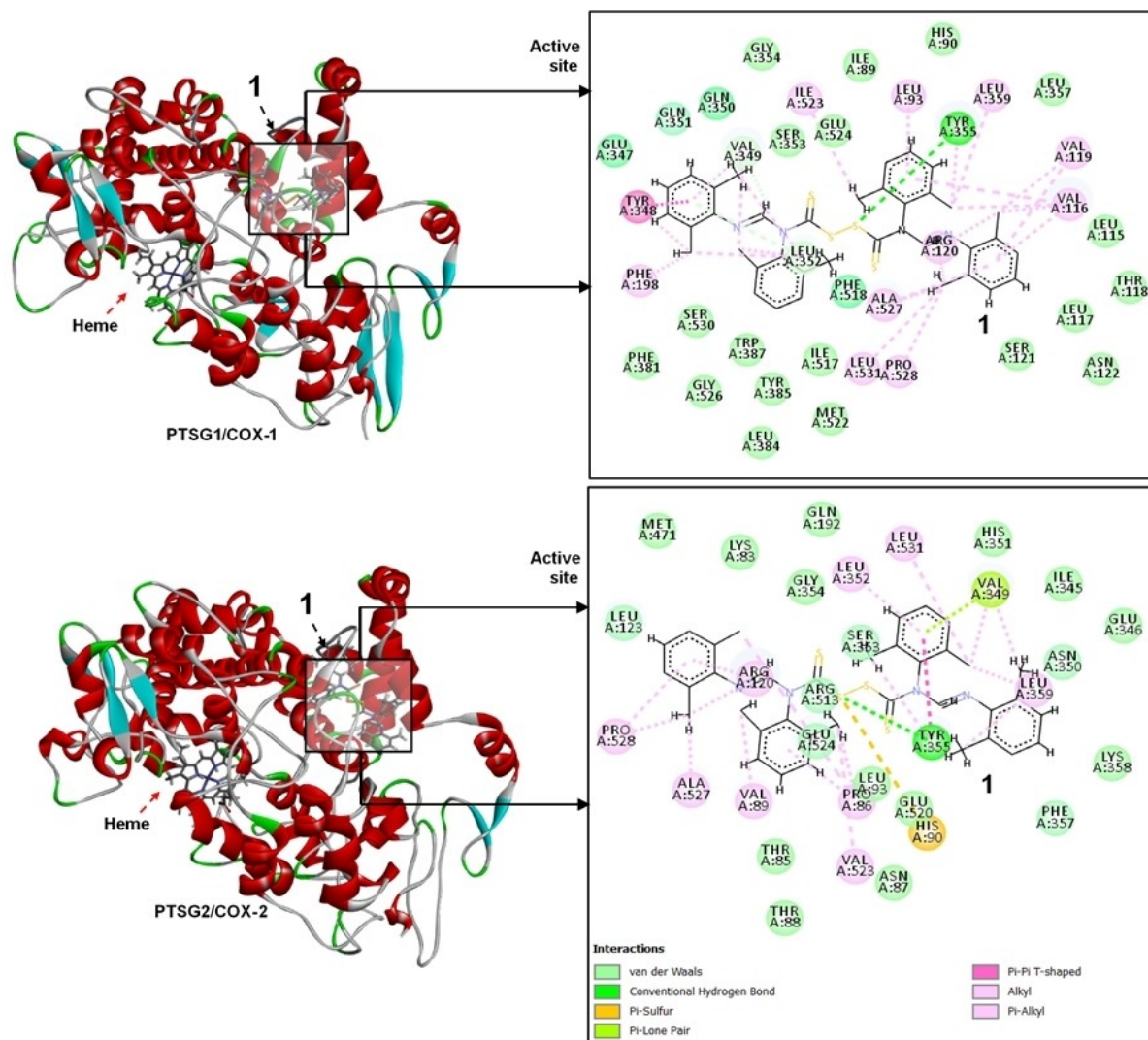
After identifying COX 1 and COX 2 as the likely targets of **1** and **4**, we predicted the interactions between these potential drug candidates and the protein targets through the established computational approaches used for protein-ligand studies. These approaches include molecular docking, molecular dynamics (MD) simulation and post-MD analyses like binding energy calculation, root mean square deviation (RMSD), root mean square fluctuation (RMSF) and radius of gyration (RoG).

2. Computational Methods

2.1. In silico Preparation of DS-Compounds, Optimization and Protein Target-Fishing

Compounds **1** to **6** were screened against a sizeable three-dimensional library of proteins to identify possible hits for each compound. Before the screening, the 2D chemical structures of **1–6** were prepared on a *Graphical User Interface* (GUI) of *MarvinSketch* software.^[18] The structures were then optimized geometrically on a *Universal Force Field* (UFF) using the steepest descent algorithm with Avogadro 1.2.0.^[19] Complete optimization of **1–6** was done using the Gaussian16 program at a B3LYP/6-311++G(d,p) theoretical level to attain the minimum energy conformation.^[20] Thereafter, the optimized compounds were saved in the appropriate Simplified Molecular-Input Line-Entry System (SMILES) in sdf and mol2 formats for subsequent *in-silico* studies.

Target-fishing was primarily carried out using the *HitPick* webserver,^[21,22] and validated using the *SwissTargetPrediction* tool.^[23] *HitPick* is a highly precise webserver for predicting possible targets for chemical compounds and integrates similarity search with methodical machine learning. These



methods are descriptive of a 2D molecular fingerprinting approach,^[24] and they entail a 1-nearest-neighbour similarity search (1NN) and a Laplacian-modified naïve Bayesian target models,^[25] which ranks potential targets based on their binding interactions with similar compounds. Moreover, the pairwise Tanimoto coefficient (Tc) determines compounds identical to each query from a cohort of known protein-ligand interactions.^[26] HitPick achieves a 60.94% sensitivity, 99.99% specificity and 92.11% precision.^[21] The SMILES format of compounds **1** to **6** was then loaded into the HitPick web server and predicted targets presented as gene symbols which were more appropriately identified in their translatable protein forms.

2.2. Retrieval of Predicted Protein Targets, Molecular Docking and Post-Docking Structural Minimization

With the potential protein targets for each query (of Section 2.1), we retrieved the correlating 3D X-ray crystal structures of the proteins from the Protein Data Bank (PDB); **1** – PTGS1/PTGS2 (5WBE/5F19),^[27,28] **2** – SCN2 A/SCN4 A (6J8E/6AGF), **3** – CAII (5N0E), **4** – PTGS1/PTGS2 (5WBE/5F19), **5** – SIGMAR1 (5HK1) and **6** – SIGMAR1 (5HK1). Before molecular docking experiments, the retrieved proteins were prepared in their monomeric forms. The preparation involved the removal of co-crystallized ions, molecules and crystal waters not relevant to this study, using the GUI of UCSF Chimera.^[29] The

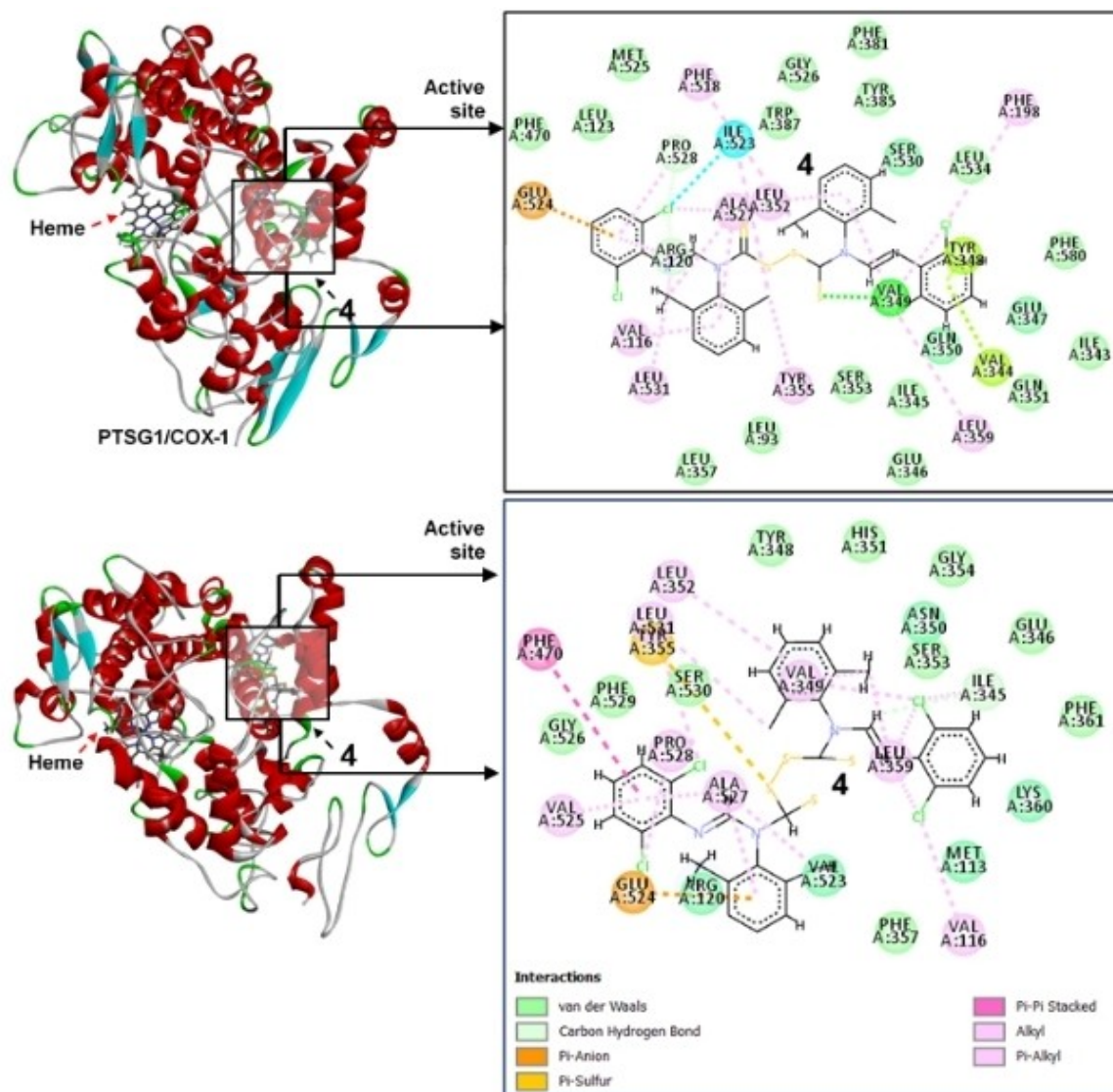


Figure 5. Dual binding interactions of **4** at the active sites of COX1 and COX2. Interaction nature and types are also shown and annotated adequately in the accompanying legend.

Molecular docking experiment into the active sites of target proteins was carried out to assess their potential as lead compounds for anticancer drug development. Compounds **1** and **4** exhibited potential dual protein selectivity towards COX1 and COX2. COX1 and COX2 are protein targets in cancer-related inflammation.^[30,31] COX 1 and COX 2 X-ray crystal structures were obtained from the protein data bank,^[32] with PDB codes 5WBE and 5F19, respectively. System preparations and visualizations were carried out on Chimera.^[29] All water and unwanted residues were removed, and hydrogen atoms were added to the proteins before docking. Molecular docking calculations were achieved using the Auto-

dockvina tool,^[33] and Gasteiger partial charges were appropriately added during docking. Autodock atom types were identified using Autodock Graphical user interface made available by MGL tools. The grid box covering the entire area occupied by the co-crystallized inhibitors was determined and had the following parameters; COX 1: $x=36.56 \text{ \AA}$, $y=161.57 \text{ \AA}$ and $z=28.45 \text{ \AA}$ for the center and $x=11.516 \text{ \AA}$, $y=11.16 \text{ \AA}$ and $z=11.33 \text{ \AA}$ for the dimension, COX 2: $x=25.28 \text{ \AA}$, $y=72.73 \text{ \AA}$ and $z=37.89 \text{ \AA}$ for the center and $x=-9.06 \text{ \AA}$, $y=15.20 \text{ \AA}$ and $z=-6.74 \text{ \AA}$ for the dimension. The exhaustiveness of the box was set at 8. The docked poses of the ligands in the binding sites of the target were generated with

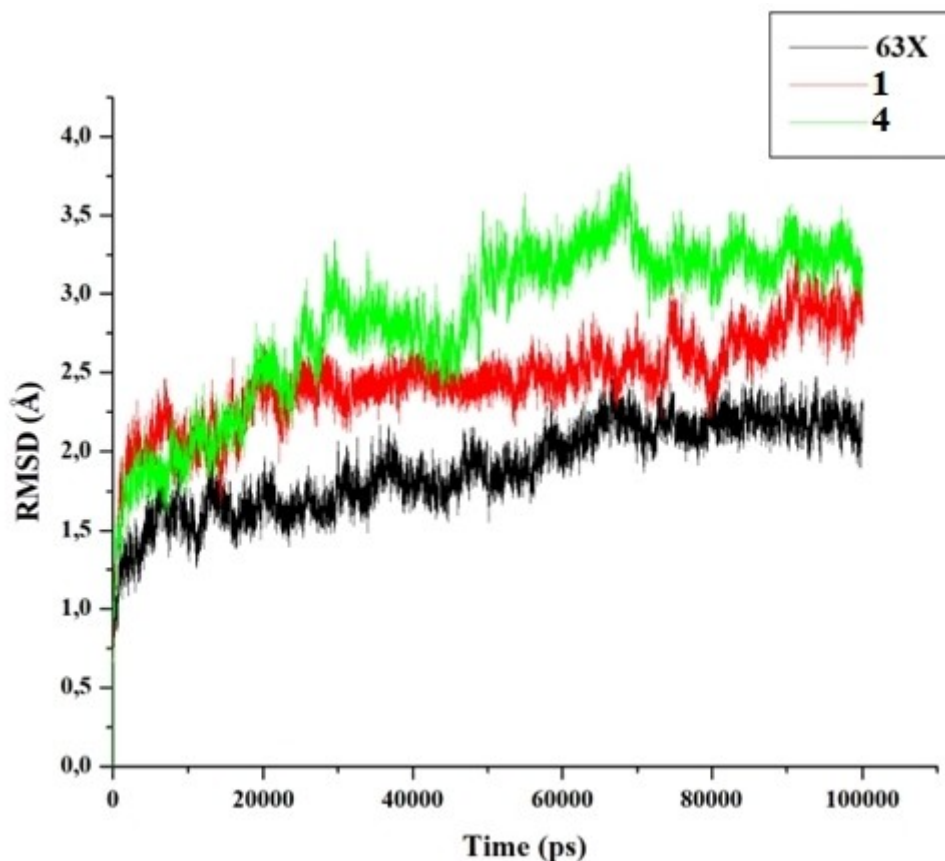


Figure 6. RMSD plot of COX1 in complex with **1**, **4** and 63X calculated from backbone alpha carbon atoms.

the Lamarckian genetic algorithm,^[34] and the docked conformations were compared with the conformation of the co-crystallized ligands. Docked conformations that were similar to the co-crystallized compounds were selected for MD simulations.

2.3. Molecular Dynamics Simulation

All MD simulations were carried out in Amber 18^[35] using the graphic processor unit (GPU) version of the Particle Ewald Molecular Dynamics (PMEMD) module.^[36] The protein structure was described with the Amber force field FF12SB. At the same time, the Gasteiger charges were used to establish the ligand parameters in Avogadro,^[19] and the antechamber module set with the Generalized Amber Force Field (GAFF). The LEAP module available in Amber 18 was employed to add hydrogen atoms and counter ions to the system. TIP3P water box was set up for the system such that the distance between the boundaries of the box and the surface of the protein was 10 Å. For the initial minimization, the restrain

potential was set at 500 kcal/mol Å⁻² for 1000 steps using the SANDER module in Amber 18. After minimization, the systems were appropriately heated from 0 to 310 K under harmonic restraint of 5 kcal/mol Å⁻² and frequency of collision of 1 ps for all solute atoms using a Langevin thermostat.^[37]

System equilibration was achieved at 310 K and isobaric condition of 1 bar without any restriction for 2 ns. Restriction on bonds having hydrogen atoms was established with the SHAKE algorithm.^[38] A 100 ns simulation at constant temperature and pressure was achieved with Berendsen barostat with a pressure-coupling constant of 2 ps. All post-MD analyses were calculated using the CPPTRAJ module of Amber 18.^[39]

2.4. Binding Free Energy Estimation

The binding free energy of each ligand-target complex was calculated using the MM/PBSA method,^[40] available in Amber 18. The MM/PBSA estimates the binding affinity of a ligand in

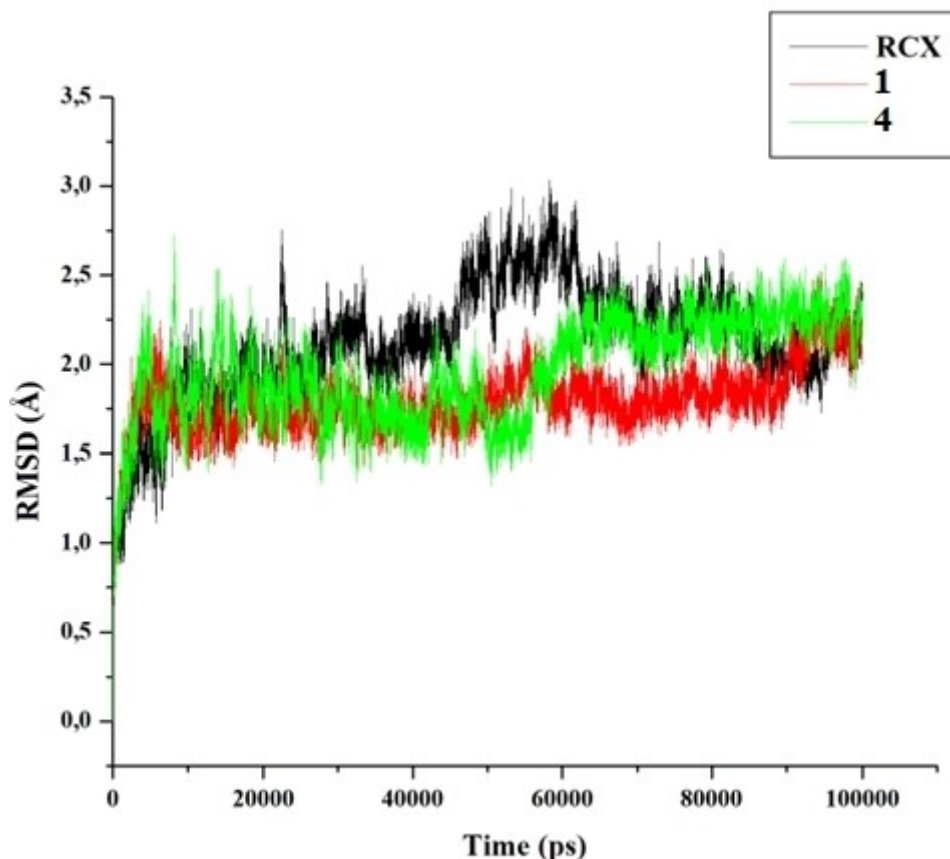


Figure 7. RMSD plot of COX2 in complex with **1**, **4** and RCX calculated from backbone alpha carbon atoms.

interaction with a macromolecule using Equations 1–4.

$$\Delta G_{\text{binding}} = G_{\text{complex}} - [G_{\text{receptor}} + G_{\text{ligand}}] \quad (1)$$

$$\Delta G_{\text{binding}} = E_{\text{MM}} + G_{\text{sol}} - T\Delta S \quad (2)$$

$$\Delta E_{\text{MM}} = E_{\text{vdW}} + E_{\text{ele}} \quad (3)$$

$$\Delta G_{\text{sol}} = G_{\text{polar}} + G_{\text{nonopolar}} \quad (4)$$

The free energy ($\Delta G_{\text{binding}}$) is the sum of the solvation free energy (G_{sol}), molecular mechanics energy (E_{MM}) and the total entropy ($-T\Delta S$) of the system. The addition of the energies from electrostatic (E_{ele}) and van der Waals (E_{vdW}) interactions gives the gas phase molecular mechanics energy (ΔE_{MM}). Polar (G_{polar}) and nonpolar ($G_{\text{nonopolar}}$) energy contributions give solvation free energy (ΔG_{sol}).^[41]

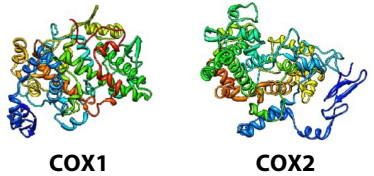
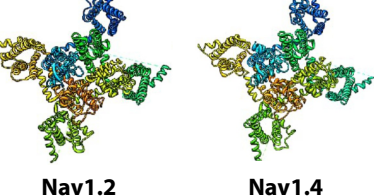
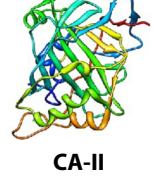
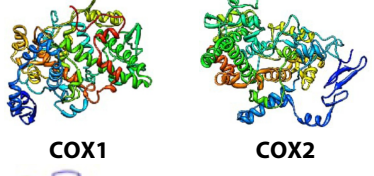
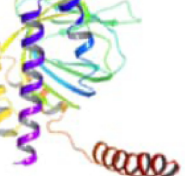
3. Results and Discussion

3.1. Identification of Potential Targets for Thiuram Disulfide **1–6**

HitPick and other integrative target-fishing methods have been previously reported and were found to be efficient in the identification of possible target proteins for new synthetic or phytochemical compounds.^[42,43] Often, a combination of these methods is employed for results that are more reliable. In this study, the HitPick webserver and SwissTargetPrediction tools were used to identify and validate potential targets for which compounds **1** to **6** might have therapeutic effects. Section 2.2, Table 1, presents compounds **1–6** along with the various predicted targets along with the 3D structures of the proteins.

Compounds **1** and **4** exhibited potential dual protein selectivity towards COX1 and COX2. COX1 and COX2 are biomolecules that have been extensively implicated in cancer-related inflammation.^[44] The two proteins genetically are associated with many neoplastic cancer types, including colorectal, pancreatic,

Table 1. Predicted protein targets, along with the 3D structures, for **1–6**.

Compounds	Predicted target	3D Structures
1 – <i>N,N'</i> -(disulfanne-1,2-dicarbonothioyl)bis(<i>N,N'</i> -bis(2,6-dimethylphenyl)formimidamide)	PTSG-1/COX1 PTSG-2/COX2	 COX1 COX2
2 – <i>N,N'</i> -(disulfanne-1,2-dicarbonothioyl)bis(<i>N,N'</i> -bis(2,6-diisopropylphenyl)formimidamide)	SCN2A/Nav 1.2 SCN4A/Nav 1.4	 Nav1.2 Nav1.4
3 – <i>N,N'</i> -(disulfanne-1,2-dicarbonothioyl)bis(<i>N,N'</i> -dimesitylformimidamide)	CA-II	 CA-II
4 – <i>N,N'</i> -(disulfanne-1,2-dicarbonothioyl)bis(<i>N,N'</i> -bis(2,6-dichlorophenyl)- <i>N</i> -(2,6-dimethylphenyl)formimidamide)	PTSG-1/COX1 PTSG-2/COX2	 COX1 COX2
5 – <i>N,N'</i> -(disulfanne-1,2-dicarbonothioyl)bis(<i>N,N'</i> -bis(2,6-dichlorophenyl)- <i>N</i> -(2,6-diisopropylphenyl)formimidamide)	SIGMAR-1	 SIGMAR-1
6 – <i>N,N'</i> -(disulfanne-1,2-dicarbonothioyl)bis(<i>N,N'</i> -bis(2,6-dichlorophenyl)- <i>N</i> -mesitylformimidamide)		SIGMAR-1

Abbreviations: COX-1→Cyclooxygenase 1, COX-2→Cyclooxygenase 2, Nav1.2→voltage-gated sodium (Na⁺) channel type II, Nav1.4→voltage-gated sodium (Na⁺) channel type IV, CA-II→Carbonic anhydrase, SIGMAR-1→Sigma-1 receptor.

breast, skin, head and haematologic cancers. Compounds **1** and **4** could be candidates for testing against the above-listed cancer types. Compound **2** dually targeted the human sodium (Na⁺) channel voltage-gated Nav1.2 and Nav1.4 variants, SCN2A and SCN4A. This is an indication of its therapeutic functionality as a potential subtype blocker for the treatment of Na_v channelopathies.^[45,46]

Compound **3** targeted the ubiquitously expressed cytosolic human Carbonic Anhydrase II isoform, hCAII,^[47] while compounds **5** and **6** targeted the human sigma-1 receptor SIGMAR 1.^[48] These are important therapeutically in several neurological dis-

orders such as depression, neuropathic pain and drug addiction.^[49] Therefore, compounds **1** and **4** potentially could have anticancer therapeutic activities compared to **2**, **3**, **5** and **6**, which seemed to target only non-carcinogenic biomolecules. Thus, their abilities as potential inhibitors of these proteins were further explored through detailed binding studies.

3.2. Molecular Docking and Elucidation of Protein-Ligand Interaction

Having identified compounds **1** and **4** as plausible inhibitors for the pro-carcinogenic COX-1 and COX-2,

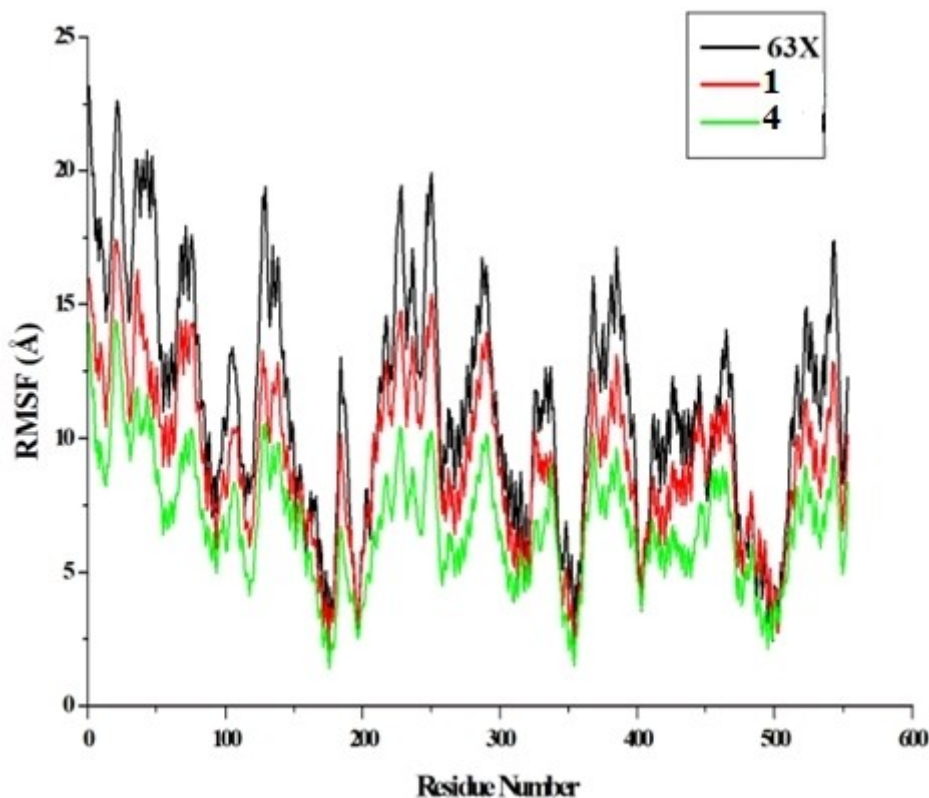


Figure 8. RMSF plot for residues of COX1 in complex with **1**, **4** and 63X (control)

the docking studies were done for only these two compounds. Optimized structures of the compounds used for docking are shown in *Figure 2*. *Figure 3*, are presented the best-docked poses and their corresponding scores. The selected poses were also superimposed with co-crystallized ligands at the active sites of target proteins to indicate a degree of accuracy and correctness in the docking method employed in this study. Findings revealed that the selected binding poses for the docked compounds exhibited at least two ring-ring alignments with ligands that were co-crystallized with COX-1 and COX-2 reported.^[50,51]

The near-crystal structure positioning of the ligands could indicate that the docking approaches were correct and relatively valid. Moreover, we observed a similar binding pattern for **1** at the active sites of both COX-1 and COX-2, complemented by the presence of strong hydrogen bonds with some key residues such as Tyr355 and Arg120. According to some previous studies, these residues play significant roles in the binding, activities and stabilization of previous COX inhibitors.^[52]

The binding pattern could suggest the ability of **1** to bind dually to both COXs since they have a highly

conserved active site. Concerning the patterns of interaction at the COX-1/2 active sites, the mid-linker sulfur atoms of **1** interact with the -OH group of Tyr355 via high-affinity hydrogen bonds, whereas a π -alkyl interaction occurs with Arg120. Thus, it shows that the sulfur-sulfur moiety in the dimer plays a role in the anticancer activity, as reported for disulfiram and indicates the anticancer potential of **1** and **4**.^[53]

In addition, several other interactions, as shown in *Figure 4* and *5*, were observed. Compound **4** showed some interactions at the active sites of COX-1 and COX-2. The binding involved strong interactions varying from hydrogen bonding to halogen bonding.

Compound **1** has binding scores of -6.1 kcal/mol and -7.2 kcal/mol with COX1 and COX2, respectively. Compound **4** has a binding score of -4.6 kcal/mol and -5.4 kcal/mol against the two proteins, respectively. These docking scores were relatively higher than those obtained for the co-crystallized ligands, as shown in *Table 2*.

Based on the docking experiments, we can safely say that **1** and **4** have similar binding/bonding patterns and modes at the active sites of COX-1 and COX-2, hence their dual selective targeting effects.

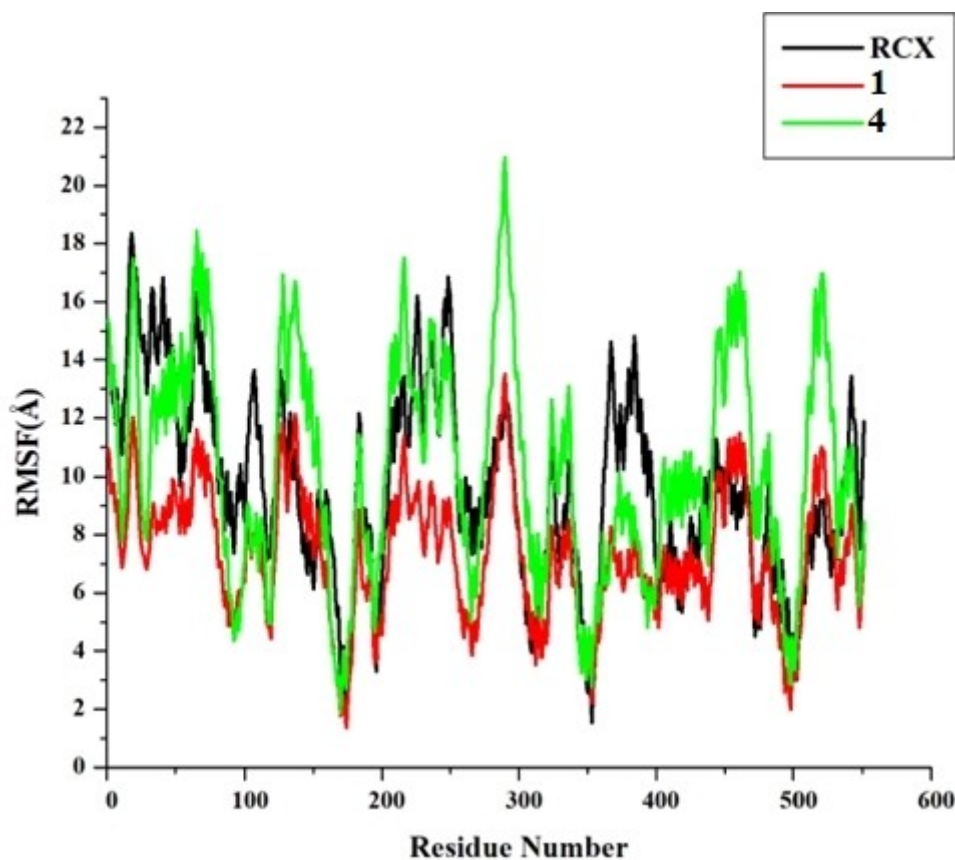


Figure 9. RMSF plot for residues of COX2 in complex with **1**, **4** and RCX (control).

Table 2. Docking scores (kcal/mol) of the compounds and the co-crystallized inhibitors of COX1 and COX2.

Complex	Docking Score
COX1- 1	−6.1
COX1- 4	−4.6
COX1-63X (control)	−4.2
COX2- 1	−7.2
COX2- 4	−5.4
COX2-RCX (control)	−5.1

3.3. System Stability

The influence of ligand binding on the stability of the protein structures was monitored over 100 ns MD trajectories. The root mean square deviation (RMSD) of the backbone atoms was calculated for each bound system to closely observe the ligands' impact on the proteins' flexibility during simulation. The compound **1** bound COX1 system showed more stability than the compound **4** bound system. The **1** bound system also showed a similar trajectory pattern with the control (63X) bound system (as shown in *Figure 6*), which may

suggest that **1** could have a similar effect on the structure of COX1 as the known inhibitor, 63X.

Against COX2, both **1** and **4** showed a more stable RMSD plot than the control compound RCX (as shown in *Figure 7*), especially from around 10 ns till the end of the simulation time. Compound **1** notably showed better stability than the rest of the systems, suggesting that the compound could probably impose more structural influence on COX2 than **4** and, more importantly, than the known inhibitor, RCX.

To further understand the overall influence of each of the ligands on the protein structures, the average RMSD values were calculated and presented in *Table 3*. For COX1, the control gave a higher average RMSD value than the **1** and **4** complexes. However, the two compounds have significantly lower average RMSD values (**1** = 1.798 Å and **4** = 1.959 Å) when compared to the control (2.120 Å) in COX2. The compounds have a varying degree of influence on the protein structures, according to the RMSD results. For COX1, the trend of influence of the compounds was control compound > **1** > **4**, while for COX2, the direction was **1** > **4** > control.

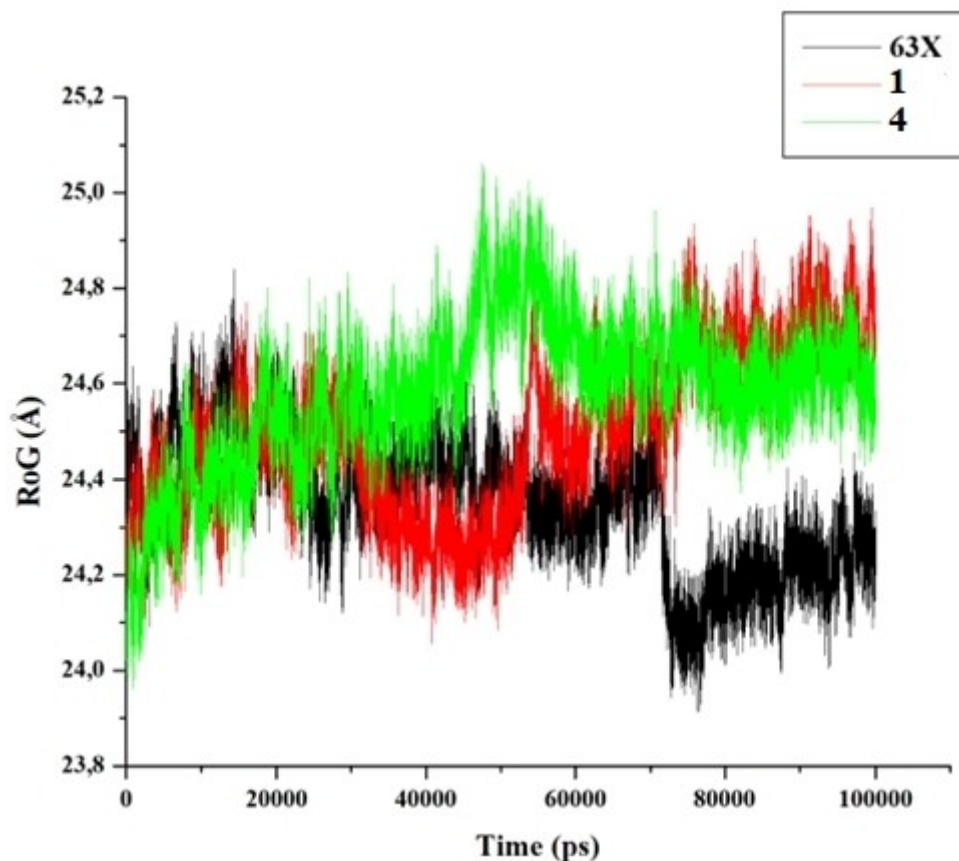


Figure 10. RoG of COX1 in complex with **1**, **4** and 63X.

Table 3. Calculated RMSD and RMSF values for each of the complexes.

COX1	Control	1	4
RMSD (Å)	1.899	2.452	2.847
RMSF (Å)	11.260	9.125	6.826
COX2			
RMSD (Å)	2.120	1.798	1.959
RMSF (Å)	9.649	7.358	10.290

3.4. Root Mean Square Fluctuation

The interactions between the ligands with the residues were observed by calculating the root mean square fluctuations of the alpha carbon atoms of the protein residues. This helps in giving insights on the changes in the flexibility of the residues upon ligand binding. *Figure 8* shows the RMSF plot for each of the bound complexes of COX1 with **1**, **4** and 63X.

All the complexes showed similar pattern of fluctuation for all the residues of COX1 with **1** and **4** systems significantly reducing the fluctuations of the

residues when compared to the control inhibitor. **4** particularly imposed the highest level of restriction on the residues of the protein, more than what was observed in **1** and 63X. *Figure 9* depicts the plot of the RMSF of COX2 residues in complex with **1**, **4** and RCX (control inhibitor). The compound **1** bound complex has the least fluctuations by the residues. The residues in compound **1** bound protein generally showed a lower degree of movement when compared to the **4** and RCX bound systems. The average RMSF for each of the complexes are also presented in *Table 3*. Both **1**-COX1 and **4**-COX2 complexes had average RMSF values (9.125 Å and 6.826 Å) that are significantly lower than the control system (11.260 Å). For the COX2 systems, the **1**-COX2 complex had the lowest average RMSF value of 7.358 Å when compared to the **4** and control bound systems with 10.290 Å and 9.649 Å, respectively. This is an indication that **1** has a significant influence on the fluctuation of the amino acid residues of COX1 and COX2, exerting more considerable influence than what was observed in the control compounds' bound systems. This observation

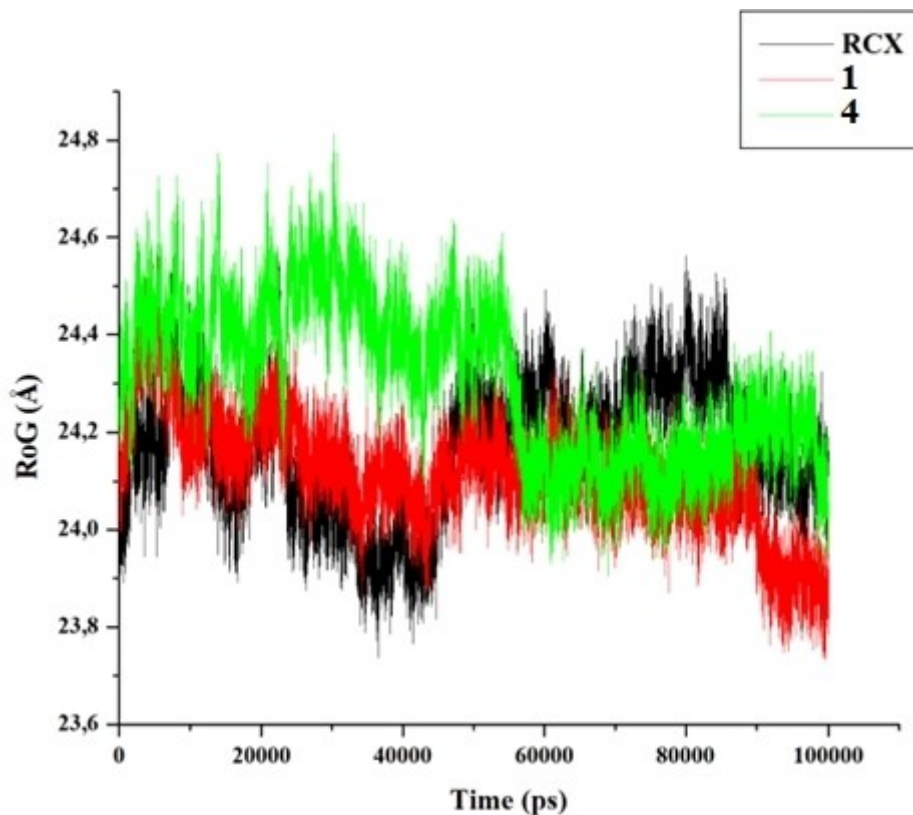


Figure 11. RoG of COX2 in complex with **1**, **4** and RCX.

indicates that **1** could be a dual target inhibitor of COX1 and COX2.

3.5. Radius of Gyration (RoG)

The radius of gyration (RoG) is a parameter used in describing the equilibrium conformation of a system over a given period.^[54] It is often used to gain insight into the compactness of protein structures and understand their flexibility under certain conditions. In this study, the RoG of the protein-ligand complexes was estimated to further understand the influence of each of the ligands on the structure of the proposed targets. *Figure 10* and *Figure 11* show the plots of the RoG for COX1 and COX2 systems, respectively. For the COX1 systems, the **4** bound complex showed the highest equilibrium with relatively more constant protein size during the simulation period when compared to **1** and 63X bound systems. COX1–**4** complex showed a slight change in size around 45–55 ps time of the simulation time. The control (63X) system significantly showed notable changes at around 70 ps but returned to equilibrium for the rest of the simulation period afterwards.

For the bound COX2, the RCX (control) and **1** systems showed a similar pattern for most of the simulation time, suggesting the two ligands could have a similar impact on the protein structure. The **4** bound complex showed a significant change in equilibrium at around 55 ps and maintained significant stability afterwards.

3.6. Binding Free Energy

The extent of interactions between the ligands and the proteins was further estimated through the binding free energy calculations. The binding free energies of the systems were calculated from the trajectories, and the results are presented in *Table 4*. Both **1** and **4** gave binding energies significantly higher than the controls in COX1 and COX2. In COX1 complexes, **1**, **4** and 63X gave binding energies of -50.64 kcal/mol, -66.51 kcal/mol and -35.95 kcal/mol, respectively. The bound COX2 systems showed -64.55 kcal/mol, -62.38 kcal/mol and -34.20 kcal/mol for **1**, **4** and RCX (control). Further analyses of the components of the ligand binding were also established. For all the inhibitors, the van der Waals interaction (ΔE_{vdw}) is the

Table 4. Components of the binding free energy (kcal/mol) of COX1 and COX2 in complex with the ligands.

Complex	ΔE_{vdw}	ΔE_{Elect}	ΔG_{Pol}	ΔG_{Nonpol}	ΔG_{Bind}
COX1- 1	-77.11 ± 3.53	-62.66 ± 9.61	89.13 ± 8.53	-9.93 ± 0.30	-50.64 ± 3.59
COX1- 4	-80.49 ± 3.51	-7.13 ± 3.00	21.10 ± 2.87	-9.64 ± 0.20	-66.51 ± 3.55
COX1-63X	-47.24 ± 2.97	-14.52 ± 4.71	25.81 ± 3.61	-6.12 ± 0.24	-35.95 ± 3.88
COX2- 1	-80.31 ± 3.28	-6.19 ± 8.77	21.95 ± 8.58	-10.13 ± 0.28	-64.55 ± 3.38
COX2- 4	-79.39 ± 3.24	-6.01 ± 2.97	23.22 ± 2.49	-9.51 ± 0.27	-62.38 ± 3.35
COX2-RCX	-42.21 ± 3.36	-22.36 ± 5.26	30.37 ± 4.02	-5.90 ± 0.27	-34.20 ± 3.96

highest contributor to the binding energies. All the ligands have hydrophobic rings as an integral part of their structures, and this explains the reason why ΔE_{vdw} has notable contributions in their binding. The presence of various heteroatoms in the ligands also makes electronic interactions quite prominent in the ligand binding, as shown in Table 4. The two compounds generally showed better binding affinity towards COX1 and COX2 better than the reference known inhibitors of these targets.

4. Conclusion

The prospects of the synthesized formamidine-based thiuram disulfides as bioactive compounds have been explored in this study through extensive computational procedures. Two compounds (**1** and **4**) out of the series were critically studied as possible anticancer drug candidates targeting COX1 and COX2 after the HitPick identified these proteins as their potential targets. The activities of **1** and **4** as possible inhibitors of COX1 and COX2 were further studied using molecular docking, molecular dynamics simulations and post-MD analyses such as binding energy calculations, RMSD, RMSF and RoG. The two compounds gave better results than the standards for COX1 (63X) and COX2 (RCX). Both **1** and **4** gave better docking scores and binding energies than the known inhibitors of the targets. The RMSD, RMSF and RoG results also suggested that these two compounds will actively bind the targets and significantly impose structural stability on the proteins. The presented results in this study showed that **1** and **4** serve as lead compounds for anticancer drug development with dual target inhibitory properties against COX1 and COX2.

Acknowledgements

The authors would like to thank the College of Agriculture, Science, and Engineering, the University of Kwazulu-Natal, Olabisi Onabanjo University and the National Research Foundation (NRF), South Africa (Grant number: 119342), for financial support.

Conflict of Interest

The authors declare no conflict of interest.

Data Availability Statement

The data that support the findings of this study are available in the supplementary material of this article.

Author Contribution Statement

Conceptualization, S.D.O., O.I.A., and B.O.; methodology, S.D.O. and O.I.A.; software, S.D.O. and O.I.A.; validation, S.D.O., O.I.A., and B.O.; formal analysis, S.D.O., O.I.A., and B.O.; resources S.D.O., O.I.A., and B.O.; data curation, S.D.O., O.I.A., and B.O.; writing – original draft preparation, S.D.O. and O.I.A.; writing – review and editing, S.D.O. O.I.A., and B.O.; visualization, S.D.O., O.I.A., and B.O.; supervision, B.O.; project administration, S.D.O., O.I.A., and B.O.; funding acquisition, S.D.O. and B.O. All authors have read and agreed to the published version of the manuscript.

References

- [1] S. D. Oladipo, F. A. Olotu, M. Soliman, C. Mocktar, B. Omondi, 'Formamidine-based thiuram disulfides: Synthesis, structural characterization, biological studies, and prelimi-

- nary cheminformatics evaluation', *J. Mol. Struct.* **2020**, *1219*, 128553–128563.
- [2] B. C. Das, N. K. Nandwana, S. Das, V. Nandwana, M. A. Shareef, Y. Das, M. Saito, L. M. Weiss, F. Almaguel, N. S. Hosmane, T. Evans, 'Boron Chemicals in Drug Discovery and Development: Synthesis and Medicinal Perspective', *Molecules* **2022**, *27*, 2615–2630.
- [3] T. L. Yusuf, S. D. Oladipo, S. A. Olagboye, S. J. Zamisa, G. F. Tolufashe, 'Solvent-free synthesis of nitrobenzyl Schiff bases: Characterization, antibacterial studies, density functional theory and molecular docking studies', *J. Mol. Struct.* **2020**, *1222*, 128857–128867.
- [4] S. D. Oladipo, C. Mocktar, B. Omondi, 'In vitro biological studies of heteroleptic Ag (I) and Cu (I) unsymmetrical N, N'-diarylformamidinium dithiocarbamate phosphine complexes; the effect of the metal center', *Arab. J. Chem.* **2020**, *13*, 6379–6394.
- [5] S. D. Oladipo, B. Omondi, C. Mocktar, 'Co(III) N,N'-diarylformamidinium dithiocarbamate complexes: Synthesis, characterization, crystal structures and biological studies', *Appl. Organomet. Chem.* **2020**, *34*, e5610–e5625.
- [6] S. D. Oladipo, B. Omondi, C. Mocktar, 'Synthesis and structural studies of nickel (II)-and copper (II)-N, N'-diarylformamidinium dithiocarbamate complexes as antimicrobial and antioxidant agents', *Polyhedron* **2019**, *170*, 712–722.
- [7] J. H. Van Drie, 'Computer-aided drug design: the next 20 years', *J. Comput.-Aided Mol. Des.* **2007**, *21*, 591–601.
- [8] S. Nag, A. T. Baidya, A. Mandal, A. T. Mathew, B. Das, B. Devi, R. Kumar, 'Deep learning tools for advancing drug discovery and development', *J. Biotechnol.* **2022**, *12*, 1–21.
- [9] V. Salmaso, S. Moro, 'Bridging Molecular Docking to Molecular Dynamics in Exploring Ligand-Protein Recognition Process: An Overview', *Front. Pharmacol.* **2018**, *9*, 923–939.
- [10] L. H. Santos, R. S. Ferreira, E. R. Caffarena, 'Integrating Molecular Docking and Molecular Dynamics Simulations', *Methods Mol. Biol.* **2019**, *2053*, 13–34.
- [11] O. I. Akinpelu, M. M. Lawal, H. M. Kumalo, N. N. Mhlongo, 'Drug repurposing: Fusidic acid as a potential inhibitor of M. tuberculosis FtsZ polymerization – Insight from DFT calculations, molecular docking and molecular dynamics simulations', *Tuberculosis* **2022**, *121*, 101920–101932.
- [12] O. I. Akinpelu, M. M. Lawal, H. M. Kumalo, N. N. Mhlongo, 'Computational studies of the properties and activities of selected trisubstituted benzimidazoles as potential anti-tubercular drugs inhibiting MTB-FtsZ polymerization', *J. Biomol. Struct. Dyn.* **2022**, *40*, 1558–1570.
- [13] O. I. Akinpelu, H. M. Kumalo, S. I. Mhlongo, N. N. Mhlongo, 'Identifying the analogs of berberine as promising anti-tubercular drugs targeting Mtb-FtsZ polymerization through ligand-based virtual screening and molecular dynamics simulations', *J. Mol. Recognit.* **2022**, *35*, e2940–e2950.
- [14] V. Salmaso, M. Sturlese, A. Cuzzolin, S. Moro, 'Exploring protein-peptide recognition pathways using a supervised molecular dynamics approach', *Structure* **2017**, *25*, 655–662.
- [15] Y. Ye, X. Wang, U. Jeschke, V. von Schonfeldt, 'COX-2-PGE-EPS in gynecology cancers', *Arch. Gynecol. Obstet.* **2020**, *301*, 1365–1375.
- [16] S. Arora, S. Gupta, S. Baishnab, 'Cyclooxygenase-1 (COX-1) inhibitors in the management of Neoplastic Disorders', *In Metastatic Diseases, Apple Academic Press* **2021**, 239–259.
- [17] A. Pannunzio, M. Coluccia, 'Cyclooxygenase-1 (COX-1) and COX-1 inhibitors in cancer. A review of oncology and medicinal chemistry literature', *Pharmaceuticals* **2018**, *11*, 101–118.
- [18] ChemAxon, <https://www.chemaxon.com/products/marvin/>. 2013.
- [19] M. D. Hanwell, D. E. Curtis, D. C. Lonie, T. Vandermeersch, E. Zurek, G. R. Hutchison, 'Avogadro: an advanced semantic chemical editor, visualization, and analysis platform', *J. Cheminf.* **2012**, *4*, 17–25.
- [20] M. Frisch, G. Trucks, H. Schlegel, G. Scuseria, M. Robb, J. Cheeseman, G. Scalmani, V. Barone, G. Petersson, H. Nakatsuji, 'Gaussian 16 Revision A 3', **2016**.
- [21] X. Liu, I. Vogt, T. Haque, M. Campillos, 'HitPick: a web server for hit identification and target prediction of chemical screenings', *Bioinformatics* **2013**, *29*, 1910–1912.
- [22] X. Wang, C. Pan, J. Gong, X. Liu, H. Li, 'Enhancing the enrichment of pharmacophore-based target prediction for the polypharmacological profiles of drugs', *J. Chem. Inf. Model.* **2016**, *56*, 1175–1183.
- [23] D. Gfeller, A. Grosdidier, M. Wirth, A. Daina, O. Michielin, V. Zoete, 'SwissTargetPrediction: a web server for target prediction of bioactive small molecules', *Nucleic Acids Res.* **2014**, *42*, 32–38.
- [24] A. Schuffenhauer, P. Floersheim, P. Acklin, E. Jacoby, 'Similarity metrics for ligands reflecting the similarity of the target proteins', *J. Chem. Inf. Comput. Sci.* **2003**, *43*, 391–405.
- [25] Nidhi, M. Glick, J. W. Davies, J. L. Jenkins, 'Prediction of biological targets for compounds using multiple-category Bayesian models trained on chemogenomics databases', *J. Chem. Inform. Model.* **2006**, *46*, 1124–1133.
- [26] P. Willett, J. M. Barnard, G. M. Downs, 'Chemical similarity searching', *J. Chem. Inf. Comput. Sci.* **1998**, *38*, 983–996.
- [27] G. Cingolani, A. Panella, M. G. Perrone, P. Vitale, G. Di Mauro, C. G. Fortuna, R. S. Armen, S. Ferorelli, W. L. Smith, A. Scilimati, 'Structural basis for selective inhibition of Cyclooxygenase-1 (COX-1) by diarylisoxazoles mofezolac and 3-(5-chlorofuran-2-yl)-5-methyl-4-phenylisoxazole (P6)', *Eur. J. Med. Chem.* **2017**, *138*, 661–668.
- [28] M. J. Lucido, B. J. Orlando, A. J. Vecchio, M. G. Malkowski, 'Crystal structure of aspirin-acetylated human cyclooxygenase-2: insight into the formation of products with reversed stereochemistry', *Biochemistry* **2016**, *55*, 1226–1238.
- [29] E. F. Pettersen, T. D. Goddard, C. C. Huang, G. S. Couch, D. M. Greenblatt, E. C. Meng, T. E. Ferrin, 'UCSF Chimera – a visualization system for exploratory research and analysis', *J. Comput. Chem.* **2004**, *25*, 1605–1612.
- [30] M. G. Perrone, A. Scilimati, L. Simone, P. Vitale, 'Selective COX-1 inhibition: A therapeutic target to be reconsidered', *Curr. Med. Chem.* **2010**, *17*, 3769–3805.
- [31] R. Ayman, A. M. Radwan, A. M. Elmetwally, Y. A. Ammar, A. Ragab, 'Discovery of novel pyrazole and pyrazolo [1,5-a]pyrimidine derivatives as cyclooxygenase inhibitors (COX-1 and COX-2) using molecular modeling simulation', *Arch. Pharm.* **2022**, p.e2200395.

- [32] H. M. Berman, J. Westbrook, Z. Feng, G. Gilliland, T. N. Bhat, H. Weissig, I. N. Shindyalov, P. E. Bourne, 'The protein data bank', *Nucleic Acids Res.* **2000**, *28*, 235–242.
- [33] O. Trott, A. J. Olson, 'AutoDock Vina: improving the speed and accuracy of docking with a new scoring function, efficient optimization, and multithreading', *J. Comput. Chem.* **2010**, *31*, 455–61.
- [34] G. M. Morris, D. S. Goodsell, R. S. Halliday, R. Huey, W. E. Hart, R. K. Belew, A. J. Olson, 'Automated docking using a Lamarckian genetic algorithm and an empirical binding free energy function', *J. Comput. Chem.* **1998**, *19*, 1639–1662.
- [35] D. Case, D. S. Cerutti, III, T. Cheatham, T. Darden, R. Duke, T. Giese, H. Gohlke, A. Goetz, D. Greene, N. Homeyer, S. Izadi, 'AMBER reference manual', *University of California* **2018**.
- [36] P. J. Needham, A. Bhuiyan, R. C. Walker, 'Extension of the AMBER molecular dynamics software to Intel's Many Integrated Core (MIC) architecture' *Comput. Phys. Commun.* **2016**, *201*, 95–105.
- [37] R. L. Davidchack, R. Handel, M. V. Tretyakov, 'Langevin thermostat for rigid body dynamics', *J. Chem. Phys.* **2009**, *130*, 234101–234116.
- [38] V. Krätzler, W. F. van Gunsteren, P. H. Hünenberger, 'A fast SHAKE algorithm to solve distance constraint equations for small molecules in molecular dynamics simulations', *J. Comput. Chem.* **2001**, *22*, 501–508.
- [39] D. R. Roe, T. E. Cheatham, 'PTRAJ and CPPTRAJ: Software for Processing and Analysis of Molecular Dynamics Trajectory Data', *J. Chem. Theory Comput.* **2013**, *9*, 3084–3095.
- [40] E. Wang, H. Sun, J. Wang, Z. Wang, H. Liu, J. Z. Zhang, T. Hou, 'End-Point Binding Free Energy Calculation with MM/PBSA and MM/GBSA: Strategies and Applications in Drug Design', *Chem. Rev.* **2019**, *119*, 9478–9508.
- [41] B. R. Miller III, T. D. McGee Jr, J. M. Swails, N. Homeyer, H. Gohlke, A. E. Roitberg, 'MMPBSA.py: an efficient program for end-state free energy calculations', *J. Chem. Theory Comput.* **2012**, *8*, 3314–3321.
- [42] J. M. Rollinger, D. Schuster, B. Danzl, S. Schwaiger, P. Markt, M. Schmidtke, J. Gertsch, S. Raduner, G. Wolber, T. Langer, H. Stuppner, 'In silico target fishing for rationalized ligand discovery exemplified on constituents of *Ruta graveolens*', *Planta Med.* **2009**, *75*, 195–204.
- [43] T. Cheng, Q. Li, Y. Wang, S. H. Bryant, 'Identifying compound-target associations by combining bioactivity profile similarity search and public databases mining', *J. Chem. Inf. Model.* **2011**, *51*, 2440–2448.
- [44] M. G. Perrone, A. Scilimati, L. Simone, P. Vitale, 'Selective COX-1 inhibition: A therapeutic target to be reconsidered', *Curr. Med. Chem.* **2010**, *17*, 3769–3805.
- [45] G. SB. Andavan, R. Lemmens-Gruber, 'Voltage-gated sodium channels: mutations, channelopathies and targets', *Curr. Med. Chem.* **2011**, *18*, 377–397.
- [46] O. K. Steinlein, 'Ion channel mutations in neuronal diseases: a genetics perspective', *Chem. Rev.* **2012**, *112*, 6334–6352.
- [47] E. Bruno, M. R. Buemi, A. Di Fiore, L. De Luca, S. Ferro, A. Angeli, R. Cirilli, D. Sadutto, V. Alterio, S. M. Monti, C. T. Supuran, 'Probing molecular interactions between human carbonic anhydrases (hCAs) and a novel class of benzene-sulfonamides', *J. Med. Chem.* **2017**, *60*, 4316–4326.
- [48] H. R. Schmidt, S. Zheng, E. Gurpinar, A. Koehl, A. Manglik, A. C. Kruse, 'Crystal structure of the human σ_1 receptor', *Nature* **2016**, *532*, 527–530.
- [49] J. L. Ortega-Roldan, F. Ossa, J. R. Schnell, 'Characterization of the human sigma-1 receptor chaperone domain structure and binding immunoglobulin protein (BiP) interactions', *J. Biol. Chem.* **2013**, *288*, 21448–21457.
- [50] H. Shen, Z. Li, Y. Jiang, X. Pan, J. Wu, B. Cristofori-Armstrong, J. J. Smith, Y. K. Chin, J. Lei, Q. Zhou, G. F. King, 'Structural basis for the modulation of voltage-gated sodium channels by animal toxins', *Science* **2018**, *362*, p.eaau2586–p.eaau2596.
- [51] X. Pan, Z. Li, Q. Zhou, H. Shen, K. Wu, X. Huang, J. Chen, J. Zhang, X. Zhu, J. Lei, W. Xiong, 'Structure of the human voltage-gated sodium channel $\text{Na}_v1.4$ in complex with β_1 ', *Science* **2018**, *362*, p.eaau2486–p.eaau2495.
- [52] B. J. Orlando, M. J. Lucido, M. G. Malkowski, 'The structure of ibuprofen bound to cyclooxygenase-2', *J. Struct. Biol.* **2015**, *189*, 62–66.
- [53] E. De Gianni, C. Fimognari, 'Anticancer Mechanism of Sulfur-Containing Compounds' *The Enzymes* **2015**, *37*, 167–192.
- [54] L. Mlu, N. S. Bogatyreva, O. V. Galzitskaia, 'Radius of gyration is indicator of compactness of protein structure', *Mol. Biol.* **2008**, *42*, 701–706.

Received September 24, 2022

Accepted December 13, 2022